Polymer 53 (2012) 130–137

Contents lists available at SciVerse ScienceDirect

Polymer

journal homepage: www.elsevier.com/locate/polymer

Controlling the ethylene polymerization parameters in iron pre-catalysts of the type 2-[1-(2,4-dibenzhydryl-6-methylphenylimino)ethyl]-6-[1-(arylimino)ethyl] pyridyliron dichloride

Weizhen Zhao [a], Jiangang Yu [a], Shengju Song [a], Wenhong Yang [a], Hao Liu [a], Xiang Hao [a], Carl Redshaw [b,**], Wen-Hua Sun [a,c,*]

[a] Key Laboratory of Engineering Plastics and Beijing National Laboratory for Molecular Sciences, Institute of Chemistry, Chinese Academy of Sciences, No. 2 Beiyijie, Zhongguancun, Beijing 100190, China
[b] School of Chemistry, University of East Anglia, Norwich, NR4 7TJ, UK
[c] State Key Laboratory for Oxo Synthesis and Selective Oxidation, Lanzhou Institute of Chemical Physics, Chinese Academy of Sciences, Lanzhou 730000, China

ARTICLE INFO

Article history:
Received 5 August 2011
Received in revised form
13 November 2011
Accepted 15 November 2011
Available online 22 November 2011

Keywords:
Ethylene polymerization
Linear polyethylene
Iron pre-catalysts

ABSTRACT

The ligand series 2-[1-(2,4-dibenzhydryl-6-methylphenylimino)ethyl]-6-[1-(arylimino)ethyl]pyridines and the iron(II) chloride complexes thereof have been synthesized and characterized by elemental and spectroscopic analyses. The molecular structures of **C1** and **C2**, determined by single-crystal X-ray diffraction analysis, confirmed a pseudo-square-pyramidal geometry at the iron center. Upon treatment with either MAO or MMAO, all iron pre-catalysts possessed good thermo-stability and exhibited high activities [up to 5.22×10^7 g mol^{-1}(Fe) h^{-1}] toward ethylene polymerization, producing highly linear polyethylene products. Optimization of the reaction parameters gave polyethylenes with narrow molecular weight distributions, indicating that single-site active species were formed; the molecular weights of the resultant polyethylenes could also be controlled.

1. Introduction

Since the initial research into the use of bis(aryliminoethyl) pyridyliron(II) dichlorides as pre-catalysts for ethylene polymerization during the late 1990s [1,2], there have been an enormous numbers of such pre-catalysts reported, as illustrated by recent review articles [3–12]. The literature has mostly focused on the use of bis(aryliminoethyl)pyridyliron(II) pre-catalysts through modifying the substituents of the parent ligand framework [13–21], or probing the catalytic intermediates with a view to establishing the identity of the active species and elucidating reaction mechanisms [22–30]. Moreover, new highly active iron pre-catalysts have been achieved by successfully designing families of imino-heterocyclic *N*-arenes, which can act as tridentate ligands [31–44] or bidentate ligands [45–47]. The deactivation of these catalytic systems and a preference for the formation of oligomers (or polyethylenes with lower molecular weights) is commonly observed for late-transition metal pre-catalysts at elevated reaction temperatures [1,48–55]. In order to enhance the thermal stability of the iron pre-catalysts, newly accessible iron complexes were developed through the design of new ligands [40], and a particularly effective strategy was achieved by employing bulky anilines within the bis(arylimino ethyl)pyridyliron(II) pre-catalyst series [20,21]. An important feature of these types of pre-catalysts is the generation of single-site active species, thereby creating polymers with narrow molecular weight distributions [1–12], however, this is often accomplished without fully understanding the factors underpinning the behavior of the pre-catalysts and without complete control over the reaction parameters. The unique property of the polyethylene products obtained via the iron pre-catalysts is their highly linear vinyl-feature [20,33–37,42], which is attracting attention in terms of further functionalization (vinyl-polyethylenes) for the production of a new generation of advanced polymers [56–58]. With regard to industrial considerations, any promising iron pre-catalysts would need to be able to act as single-site active species in producing polyethylenes with a narrow molecular weight distribution. Furthermore, suitable reaction parameters are critically important to maintain the stability of the

* Corresponding author. Key Laboratory of Engineering Plastics and Beijing National Laboratory for Molecular Sciences, Institute of Chemistry, Chinese Academy of Sciences, No. 2 Beiyijie, Zhongguancun, Beijing 100190, China. Tel.: +86 10 62557955; fax: 86 10 62618239.
** Corresponding author. Tel.: +44 (0)1603 593137; fax: +44 (0)1603 592003.
E-mail addresses: carl.redshaw@uea.ac.uk (C. Redshaw), whsun@iccas.ac.cn (W.-H. Sun).

0032-3861/$ – see front matter © 2011 Elsevier Ltd. All rights reserved.
doi:10.1016/j.polymer.2011.11.024

active species, in particular the operational parameters of ethylene pressure and reaction temperature.

In our recent work on the variation of the unsymmetrical bis(iminoethyl)pyridyliron type pre-catalysts, the catalytic system achieved good thermo-stability and high activity in ethylene polymerization in several cases, producing polyethylenes with narrow molecular weight distributions (as low as 2.0) [20]. Beyond overcoming the problems associated with the thermo-stability of an active catalytic system, another demanding issue is the tailoring of the polyethylene products in order to match the required application [56–58]. Besides the reaction of two different anilines with 2,6-diacetylpyridine to form a series of unsymmetrical bis(iminoethyl)pyridines [20], there are no reports dealing with unsymmetrical bis(iminoethyl)pyridines derived from a bulky unsymmetrical aniline and a second common aniline. As a consequence, 2,4-dibenzhydryl-6-methylaniline was prepared and used instead of 2,6-dibenzhydryl-4-methylaniline, and a series of 2-[1-(2,4-dibenzhydryl-6-methylphenylimino)ethyl]-6-[1-(arylimino) ethyl]pyridines and the iron dichloride complexes thereof were synthesized and characterized. Upon variation of the reaction parameters, polyethylenes with different molecular weights and molecular weight distributions, particularly with quite narrow molecular weight distributions, were obtained. Herein, the preparation and characterization of the title iron pre-catalysts are reported, and the reaction parameters and resultant polyethylenes are presented and discussed in detail.

2. Experimental

2.1. General considerations

All air- and/or moisture-sensitive operations were carried out in an atmosphere of nitrogen using standard Schlenk techniques. The solvents were purified and dried under nitrogen by conventional methods prior to use unless otherwise stated. Methylaluminoxane (a, 1.46 M solution in toluene) and modified methylaluminoxane (MMAO, 1.93 M in heptane, 3A) were purchased from Akzo Nobel Corp. High-purity ethylene was purchased from Beijing Yanshan Petrochemical Co. and used as received. Other reagents were purchased from Aldrich, Acros, or local suppliers. NMR spectra were recorded on Bruker DMX 400/600 MHz instrument at ambient temperature using TMS as an internal standard. IR spectra were recorded on a Perkin-Elmer System 2000 FT-IR spectrometer. Elemental analysis was carried out using a Flash EA 1112 micro-analyzer. Molecular weights and molecular weight distribution (MWD) of polyethylenes were determined by a PL-GPC220 at 150 °C, with 1,2,4-trichlorobenzene as the solvent. DSC trace and melting points of polyethylene were obtained from the second scanning run on Perkin-Elmer DSC-7 at a heating rate of 10 °C/min.

2.2. Preparation of the ligands

2.2.1. Synthesis of 2-acetyl-6-(1-(2,4-dibenzhydryl-6-methylphenyl imino)ethyl)-pyridine

A mixture of 2,4-dibenzhydryl-6-methylaniline (8.52 g, 20 mmol), 2,6-diacetylpyridine (3.26 g, 20 mmol) and a catalytic amount of *p*-toluenesulfonic acid in toluene (150 mL) was refluxed for 6 h. After solvent evaporation at reduced pressure, the crude product was purified by silica-based column chromatography (Vpetroleum ether:Vethyl acetate = 30:1) to afford the yellow product (44% yield). Mp: 134–136 °C. FT-IR (KBr, cm^{-1}): 3024, 2919, 2160, 2030, 1977, 1702, 1642 ($\nu_{C\equiv N}$), 1493, 1466, 1365, 1235, 1118, 1076, 1031, 819, 765, 739, 698 ^{1}H NMR (400 MHz, $CDCl_3$, TMS): δ 8.45 (d, 1H, J = 7.9 Hz, -Py), 8.10 (d, 1H, J = 3.8 Hz, -Py), 7.92 (t, 1H, J = 4.0 Hz, -Py),7.24 (s, 1H, -Ph), 7.22 (s, 1H, -Ph), 7.20–7.14 (m, 5H, -Ph), 7.10–7.06 (m, 8H, -Ph), 6.97 (d, 2H, J = 7.3 Hz, -Ph), 6.90 (d, 2H, J = 4.01 Hz, -Ph), 6.86 (s, 1H, -Ph), 6.61 (s, 1H, -Ph), 5.41 (s, 1H, −CH−), 5.37 (s, 1H, −CH−), 2.71(S, 3H, $-CH_3$), 1.93 (S, 3H, $-CH_3$), 1.57 (S, 3H, $-CH_3$). ^{13}C NMR (100 MHz, $CDCl_3$, TMS): δ 200.3, 168.4, 155.6, 152.5, 145.9, 143.5, 142.7, 137.3, 133.2, 129.9, 129.6, 129.5, 128.9, 128.3, 128.1, 126.2, 126.1, 124.6, 122.6, 56.4, 52.5, 25.8, 18.1, 16.5.

2.2.2. 2-(1-(2,4-dibenzhydryl-6-methylphenylimino)ethyl)-6-(1-(2, 6-imethylphenylimino)ethyl)pyridine (*L1*)

A solution of 2-acetyl-6-(1-(2,6-diphenylmethyl-4-methyl imino)ethyl)pyridine (1.14 g, 2.0 mmol), 2,6-dimethylaniline (0.24, 2.0 mmol) and a catalytic amount of *p*-toluenesulfonic acid in toluene (50 mL) was mixed and refluxed for 3 h. The solution was evaporated at reduced pressure. The residual solids were further purified by alumina-based column chromatography (Vpetroleum ether:Vethyl acetate = 50:1) to afford yellow **L1** (20.5% yield). Mp: 203–204 °C. FT-IR (KBr, cm^{-1}): 3061, 3023,2917, 2162, 2027, 1979, 1640 ($\nu_{C\equiv N}$), 1494, 1467, 1367, 1237, 1125, 1077, 818, 765, 739, 700. ^{1}H NMR (400 MHz, $CDCl_3$, TMS): δ 8.43 (d, 1H, J = 7.7 Hz, -Py), 8.35 (d, 1H, J = 7.8 Hz, -Py), 7.88 (t, 1H, J = 7.80 Hz, -Py), 7.25-7.22 (m,4H, -Ph), 7.17–7.15 (m, 5H, -Ph), 7.09–7.06 (m, 9H, -Ph), 6.99–6.96 (m, 2H, -Ph), 6.94–6.91 (m, 2H, -Ph), 6.86 (s, 1H, -Ph), 6.62 (s, 1H, -Ph), 5.41 (s, 2H, −CH−), 2.16 (s, 3H, $-CH_3$), 2.08 (s, 3H, $-CH_3$), 2.03 (s, 3H, $-CH_3$), 1.94 (s, 3H, $-CH_3$), 1.61 (s, 3H, $-CH_3$). ^{13}C NMR (100 MHz, $CDCl_3$, TMS): δ 168.9, 167.4, 155.2, 155.0, 148.9, 146.7, 143.6, 142.9, 138.1, 136.8, 133.2, 130.0, 129.5, 129.0, 128.2, 126.2 126.1, 125.6, 123.2, 122.3, 122.2, 56.5, 21.4, 18.1, 16.7, 17.0, 16.6.

2.2.3. 2-(1-(2,4-dibenzhydryl-6-methylphenyimino)ethyl)-6-(1-(2, 6-diethylphenylimino)ethyl)pyridine (*L2*)

Using the same procedure as for the synthesis of **L1**, **L2** was obtained as a yellow powder in 19.1% yield. Mp: 203–204 °C. FT-IR (KBr, cm^{-1}): 3058, 3027, 2960, 2928, 2162, 2033, 1980, 1638 ($\nu_{C\equiv N}$), 1494, 1450, 1363, 1245, 1120, 1078, 761, 698. ^{1}H NMR (400 MHz, $CDCl_3$, TMS): δ 8.42 (d, 1H, J = 7.8 Hz, -Py), 8.35 (d, 1H, J = 7.9 Hz, -Py), 7.89 (t, 1H, J = 7.7 Hz, -Py), 7.25–7.22 (m, 6H, -Ph), 7.17–7.14 (m, 4H, -Ph), 7.10–7.02 (m, 10H, -Ph), 6.99–6.96 (m, 2H, -Ph), 6.94–6.91 (m, 2H, -Ph), 6.86 (s, 1H, -Ph), 6.62 (s, 1H, -Ph), 5.41 (s, 2H, −CH−), 2.48–2.28 (m, 4H, −CH−), 2.17 (s, 3H, $-CH_3$), 1.95 (s, 3H, $-CH_3$), 1.61 (s, 3H, $-CH_3$), 1.18 (t, 3H, J = 7.52 Hz, $-CH_3$), 1.13 (t, 3H, J = 7.49 Hz, $-CH_3$). ^{13}C NMR (100 MHz, $CDCl_3$, TMS): δ 168.9, 167.1, 155.3, 155.2, 148.0, 146.7, 143.6, 142.9, 136.9, 133.2, 131.3, 130.0, 129.5, 129.0, 128.3, 128.1, 126.2, 126.1, 125.2, 123.5, 122.3, 122.02, 52.4, 24.8, 24.7, 18.2, 16.9, 13.9.

2.2.4. 2-(1-(2,4-dibenzhydryl-6-methylphenyimino)ethyl)-6-(1-(2,6-diisopropyl-phenylimino)ethyl)pyridine (*L3*)

Using the same procedure as for the synthesis of **L1**, **L3** was obtained as a yellow powder in 22.1% yield. Mp: 165–167 °C. FT-IR (KBr, cm^{-1}): 3066, 3021, 2966, 2901, 2017, 1967, 1642 ($\nu_{C\equiv N}$), 1492, 1453, 1361, 1238, 1122, 829, 762, 698. ^{1}H NMR (400 MHz, $CDCl_3$, TMS): δ 8.42 (d, 1H, J = 8.0 Hz, -Py), 8.34 (d, 1H, J = 4.0 Hz, -Py), 7.89 (t, 1H, J = 8.0 Hz, -Py), 7.23 (d, 5H, J = 4.0 Hz, -Ph), 7.17 (t, 6H, J = 4.0 Hz, -Ph), 7.12–7.06 (m, 8H, -Ph), 6.98 (d, 2H, J = 4.0 Hz, -Ph), 6.92 (t, 2H, J = 4.0 Hz, -Ph), 6.86 (s, 1H, -Ph), 6.62 (s, 1H, -Ph), 2.83–2.71 (m, 2H, −CH−), 2.18 (s, 3H, $-CH_3$), 1.95 (s, 3H, $-CH_3$), 1.63 (s, 3H, $-CH_3$), 1.19 (d, 6H, J = 8.0 Hz, $-CH_3$), 1.14 (d, 6H, J = 6.8 Hz, $-CH_3$). ^{13}C NMR (100 MHz, $CDCl_3$, TMS): δ 168.9, 167.1, 155.3, 155.2, 146.7, 146.6, 143.6, 142.9, 136.9, 135.9, 133.2, 131.7, 130.0, 129.5, 129.0, 128.1, 126.2, 126.1, 123.7, 123.1, 122.2, 122.0, 52.4, 28.4, 23.4, 23.1, 18.2, 17.3, 16.1.

2.2.5. 2-(1-(2,4-dibenzhydryl-6-methylphenyimino)ethyl)-6-(1-(2,4,6-trimethyl-phenylimino)ethyl)pyridine (*L4*)

Using the same procedure as for the synthesis of **L1**, **L4** was obtained as a yellow powder in 13.5% yield. Mp: 213–215 °C. FT-IR (KBr,

cm^{-1}): 3058, 3024, 2915, 2172, 2016, 1967, 1641 ($\nu_{C\equiv N}$), 1493, 1450, 1364, 1214, 1120, 740, 698. ^{1}H NMR (400 MHz, $CDCl_3$, TMS): δ 8.44 (d, 1H, J = 7.8 Hz, -Py), 8.35 (d, 1H, J = 7.8 Hz, -Py), 7.89 (t, 1H, J = 7.8 Hz, -Py), 7.27–7.24 (m, 5H, -Ph), 7.20–7.15 (m, 5H, -Ph), 7.13–7.07 (m, 7H, -Ph), 7.00 (d, 2H, J = 7.5 Hz, -Ph), 6.94–6.90 (m, 4H, -Ph), 6.87 (s, 1H, -Ph), 6.63 (s, 1H, -Ph), 5.43 (s, 2H, –CH–), 2.31 (s, 3H, $-CH_3$), 2.17 (s, 3H, $-CH_3$), 2.05 (s, 3H, $-CH_3$), 2.01 (s, 3H, $-CH_3$), 1.95 (s, 3H, $-CH_3$), 1.62 (s, 3H, $-CH_3$). ^{13}C NMR (100 MHz, $CDCl_3$, TMS): δ 168.9, 167.6, 155.2, 146.4, 143.8, 142.8, 136.7, 132.3, 131.7, 130.0, 129.6, 128.8, 128.7, 128.4, 128.1, 126.2, 126.1, 125.4, 122.2, 52.4, 20.9, 18.0, 16.7, 16.5.

2.2.6. 2-(1-(2,4-dibenzhydryl-6-methylphenyimino)ethyl)-6-(1-(2,6-diethyl-4-methylphenylimino)ethyl)pyridine (*L5*)

Using the same procedure as for the synthesis of **L1**, **L5** was obtained as a yellow powder in 32.2% yield. Mp: 200–202 °C. FT-IR (KBr, cm^{-1}): 3060, 2963, 2929, 2870, 2158, 2030, 1967, 1644 ($\nu_{C\equiv N}$), 1494, 1452, 1366, 1211, 1121, 735, 699. ^{1}H NMR (400 MHz, $CDCl_3$, TMS): δ 8.41 (d, 1H, J = 7.8 Hz, -Py), 8.34 (d, 1H, J = 7.8 Hz, -Py), 7.88 (t, 1H, J = 7.8 Hz, -Py), 7.25–7.22 (m, 6H, -Ph), 7.19–7.15 (m, 4H, -Ph), 7.12–7.07 (m, 7H, -Ph), 6.99 (s, 1H, -Ph), 6.97 (s, 1H, -Ph), 6.93 (s, 3H, -Ph), 6.85 (s, 1H, -Ph), 6.62 (s, 1h, -Ph), 2.46–2.24 (m, 4H, $-CH_2-$), 2.34 (s, 3H, $-CH_3$), 2.16 (s, 3H, $-CH_3$), 1.94 (s, 3H, $-CH_3$), 1.61 (s, 3H, $-CH_3$), 1.16 (t, 3H, J = 7.4 Hz, $-CH_3$), 1.11 (t, 3H, J = 7.5 Hz, $-CH_3$). ^{13}C NMR (100 MHz, $CDCl_3$, TMS): δ 170.1, 167.4, 155.2, 146.2, 143.8, 142.8, 136.7, 132.5, 132.3, 131.7, 130.0, 129.6, 128.8, 128.3, 128.1, 126.8, 126.2, 126.1, 122.3, 121.9, 52.2, 24.7, 21.4, 21.1, 17.0, 16.8, 14.0.

2.3. Synthesis of iron complexes (*C1*–*C5*)

The complexes **C1**–**C5** were synthesized by the reaction of $FeCl_2\cdot 4H_2O$ with the corresponding ligands in ethanol. A typical synthetic procedure for **C1** can be described as follows: The ligand **L1** (151 mg, 0.22 mmol) and $FeCl_2\cdot 4H_2O$ (79.5 mg, 0.20 mmol) were added to a Schlenk tube, followed by the addition of freshly distilled ethanol (5 mL) with rapid stirring at room temperature. The solution turned blue immediately, and a blue precipitate was formed. The reaction mixture was stirred for 8 h, and then the precipitate was washed with diethyl ether (3 × 5 mL) and dried to give the product as a blue powder in 88.7% yield. FT-IR (KBr, cm^{-1}): 3061, 3027, 2968, 2915, 2876, 2162, 2030, 1991, 1967, 1584 ($\nu_{C\equiv N}$), 1495, 1450, 1368, 1259, 1213, 1032, 818, 770, 741, 702. Anal. Calcd for $C_{52}H_{49}Cl_2FeN_3$ (843): C, 74.11; H, 5.86; N, 4.99. Found: C, 74.01; H, 5.69; N, 5.12. Data for **C2** are as follows. Yield: 75%. FT-IR (KBr, cm^{-1}): 3058, 3026, 2968, 2915, 2868, 2360,2342, 1961, 1581 ($\nu_{C\equiv N}$), 1494, 1446, 1371, 1273, 1212, 1078, 1030, 803, 779, 750, 698. Anal. Calcd for $C_{52}H_{49}Cl_2FeN_3$ (843): C, 74.11; H, 5.86; N, 4.99. Found: C, 74.01; H, 5.69; N, 5.12. Data for **C3** are as follows. Yield: 85%. FT-IR (KBr, cm^{-1}): 3061, 3023, 2970, 2865, 2161, 2030, 2012, 1978, 1962, 1586 ($\nu_{C\equiv N}$), 1494, 1450, 1371, 1258, 1211, 1079, 1033, 783, 744, 700. Anal. Calcd for $C_{54}H_{53}Cl_2FeN_3$ (871): C, 74.48; H, 6.13; N, 4.83. Found: C, 74.21; H, 6.03; N, 4.99. Data for **C4** are as follows. Yield: 85.9%. FT-IR (KBr, cm^{-1}): 3436, 3056, 3041, 3026, 2972, 2901, 2030, 1973, 1963, 1580 ($\nu_{C\equiv N}$), 1494, 1445, 1368, 1219, 1077, 1066, 1037, 745, 698. Anal. Calcd for $C_{51}H_{47}Cl_2FeN_3$ (829): C, 73.92; H, 5.72; N, 5.07. Found: C, 73.66; H, 5.42; N, 5.01. Data for **C5** are as follows. Yield: 78.5%. FT-IR (KBr, cm^{-1}): 3062, 3028, 2967, 2867, 2030, 2006, 1976, 1962, 1580 ($\nu_{C\equiv N}$), 1494, 1447, 1370, 1271, 1216, 1078, 1034, 868, 806, 738, 703. Anal. Calcd for $C_{53}H_{51}Cl_2FeN_3$ (829): C, 74.30; H, 6.00; N, 4.90. Found: C, 73.98; H, 5.83; N, 5.12.

2.4. Procedures for ethylene polymerization

2.4.1. Ethylene polymerization at 1 atm of ethylene pressure

Ethylene polymerization at 1 atm of ethylene pressure was carried out as follows: The catalyst precursor was dissolved in toluene in a Schlenk tube and the reaction solution was stirred at 1 atm of ethylene with the reaction temperature set as required. The reaction was initiated by adding the desired amount of co-catalyst. After the desired period of time, the reactor was cooled in ice-water bath, and resultant reaction mixture was then quenched with HCl–acidified ethanol (5%). The precipitated polyethylene was filtered, washed with ethanol, dried in a vacuum at 60 °C until constant weight.

2.4.2. Ethylene polymerization at 10 atm of ethylene pressure

A stainless steel autoclave (250 mL) equipped with a mechanical stirrer and a temperature controller was heated in vacuum at 80 °C and recharged with ethylene three times, then cooled to room temperature under ethylene atmosphere. A toluene solution containing the iron complex was inserted to the reactor by syringe; after adapting the reaction temperature as required, the required amount of co-catalyst (with total 100 mL volume maintained through adding toluene) was added, then the autoclave was immediately pressurized to 10 atm and kept constant during the reaction with feeding ethylene. After the required time, the ethylene feed was stopped, and the autoclave was placed in a water-ice bath for 1 h. The resultant mixture was poured into 10% HCl–ethanol solution, and the polymer was collected and washed with ethanol several times and dried under vacuum to constant weight.

2.5. X-ray structure determination

Single-crystal X-ray diffraction for **C1** and **C2** was carried out on a Rigaku R-AXIS Rapid IP diffractometer with graphite-monochromated Mo Kα radiation (λ = 0.71073 Å) at 173(2) K. Intensities were corrected for Lorentz and polarization effects and empirical absorption. The structures were solved by direct methods and refined by full-matrix least-squares on F^2. All hydrogen atoms were placed in calculated positions. Structure solution and refinement were performed by using the SHELXL-97 package [59]. Crystal data and processing parameters for complexes **C1** and **C2** are summarized in Table 1.

3. Results and discussion

3.1. Preparation and characterization of the iron complexes

Employing our previous procedure, but using 2,4-dibenzhydryl-6-methyl phenylamine instead of 2,6-dibenzhydryl-4-methylphenylamine [20], a series of unsymmetrical 2-[1-(2,4-dibenzhydryl-6-methylphenylimino)ethyl]-6-[1-(arylimino)ethyl] pyridines was prepared in a two-step reaction (Scheme 1). Subsequent treatment with one equivalent of $FeCl_2\cdot 4H_2O$ in ethanol afforded the corresponding iron dichloride complexes in good yields (Scheme 1). All organic compounds were characterized by elemental analysis, FT-IR spectra and NMR spectroscopic measurements, whilst the title iron complexes were characterized by elemental analysis and FT-IR spectra, and the molecular structures of the complexes **C1** and **C2** were confirmed by single-crystal X-ray diffraction.

Single crystals of the complexes **C1** and **C2** suitable for X-ray diffraction analysis were obtained by slow diffusion of diethyl ether into their dichloromethane solution under a nitrogen atmosphere. The ORTEP drawings of complexes **C1** and **C2** are shown in Figs. 1 and 2, respectively, together with selected bond lengths and angles. The coordination geometry of both complexes can be best described as a pseudo-square-pyramidal geometry with three nitrogen atoms N(1), N(2) and N(3) and one chlorine atom Cl(1) forming the basal square plane, with the iron atom lying out of the

Table 1
Crystal data and structure refinement for **C1** and **C2**.

	C1	**C2**
CCDC No.	838017	838018
Empirical formula	$C_{50}H_{45}Cl_2N_3Fe$	$C_{104}H_{98}Cl_4N_6Fe_2$
Fw	814.64	1685.38
T (K)	173(2)	173(2)
Wavelength (Å)	0.71073	0.71073
Cryst syst	Triclinic	Triclinic
Space group	P-1	$P2_1/c$
a (Å)	9.6322(19)	15.189(3)
b (Å)	15.298(3)	33.893(7)
c (Å)	16.352(5)	20.168(4)
α (°)	82.27(3)	90
β (°)	83.38(3)	110.96 (3)
γ (°)	77.02(3)	90
V (Å3)	2317.7(8)	9696(3)
Z	2	4
D calcd (mg m^{-3})	1.167	1.155
μ (mm^{-1})	0.475	0.457
F(000)	852	3536
Cryst size (mm)	0.35 × 0.12 × 0.09	0.23 × 0.18 × 0.03
θ range (°)	1.37–25.35	1.20–25.34
Limiting indices	$-7 \le h \le 11$	$-16 \le h \le 18$
No. of rflns collected	13,407	34,789
No. unique rflns [R(int)]	8355 (0.0754)	17,557 (0.0620)
Completeness to θ (%)	98.3%	98.9%
Abs corr	None	None
Data/restraints/params	8355/0/505	17557/0/1047
Goodness of fit on F^2	1.082	1.039
Final R indices [$I > 2\sigma(I)$]	$R^1 = 0.1138$	$R^1 = 0.0991$
R indices (all data)	$R^1 = 0.1642$	$R^1 = 0.1499$
Largest diff peak and hole (e Å-3)	0.526 and −0.513	0.830 and −0.414

plane at 0.554 Å for **C1** and 0.674 Å for **C2** with the N(1)-Fe1-N(2) angle as 73.22°(**C1**) and 72.53°(**C2**), N(2)-Fe1-N(3) angle as 73.50°(**C1**) and 73.88°(**C2**). The Fe-N bond lengths were similar to their analogous complexes, and were unexceptional [20].

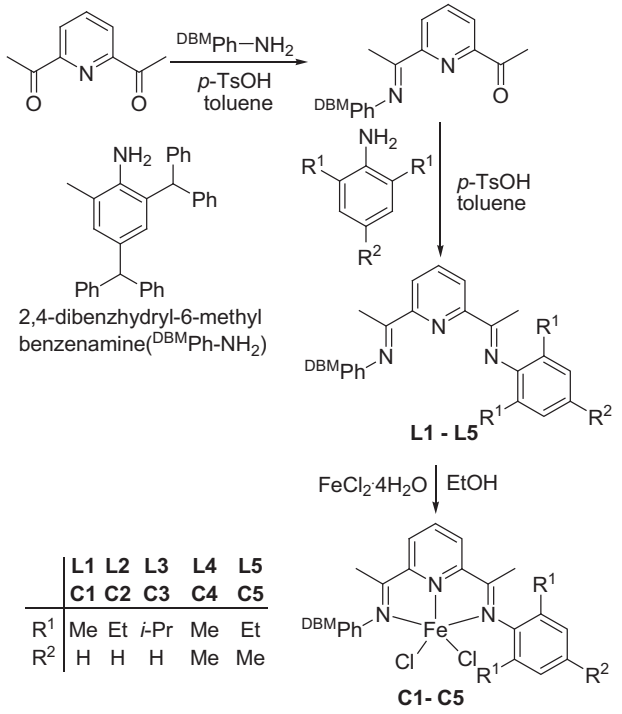

	L1	L2	L3	L4	L5
	C1	C2	C3	C4	C5
R^1	Me	Et	*i*-Pr	Me	Et
R^2	H	H	H	Me	Me

Scheme 1. Synthesis of ligands (**L1**–**L5**) and iron complexes (**C1**–**C5**).

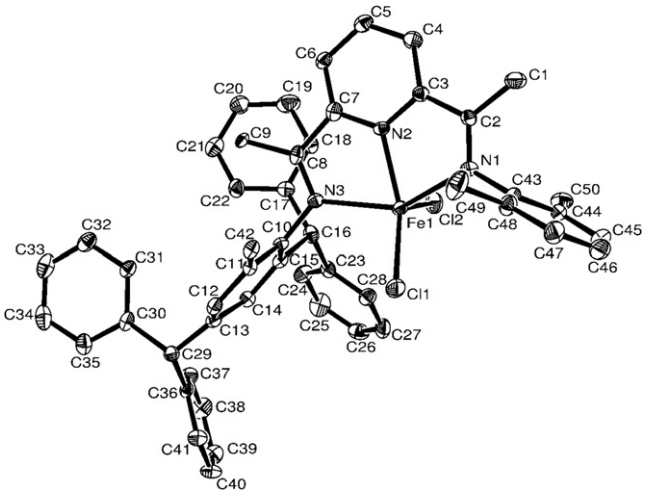

Fig. 1. ORTEP drawing of complex **C1** with thermal ellipsoids at 30% probability level. Hydrogen atoms have been omitted for clarity. Selected bond length (°) and selected bond angles (Å): Fe(1)-N(1) 2.230(6), Fe(1)-N(2) 2.086(5), Fe(1)-N(3) 2.256(5), Fe(1)-Cl(1) 2.263(2), Fe(1)-Cl(2) 2.319(2), N(1)-C(2) 1.274(9), N(1)-C(43) 1.438(8), N(2)-C(3) 1.341(9), N(2)-C(7) 1.363(9), N(3)-C(8) 1.277(9), N(3)-C(10) 1.475(9), N(2)-Fe(1)-N(1) 73.2(2), N(2)-Fe(1)-Cl(1) 143.39(18), N(3)-Fe(1)-Cl(1) 98.15(16), N(2)-Fe(1)-N(3) 73.5(2), N(1)-Fe(1)-N(3) 144.7(2), N(1)-Fe(1)-Cl(1) 101.59(17), N(2)-Fe(1)-Cl(2) 95.76(17), N(3)-Fe(1)-Cl(2) 98.91(16), Cl(1)-Fe(1)-Cl(2) 120.84(10), N(1)-Fe(1)-Cl(2) 95.64(17).

3.2. Ethylene polymerization

Various alkylaluminum reagents were screened as suitable co-catalysts, and high activities for the title iron pre-catalysts were observed when using the co-catalysts methylaluminoxane (MAO) and modified methylaluminoxane (MMAO). The catalytic activities of the iron pre-catalysts and the properties of the resultant polyethylenes could be adapted by changing the reaction parameters including ethylene pressure, molar ratio of aluminum to iron, and

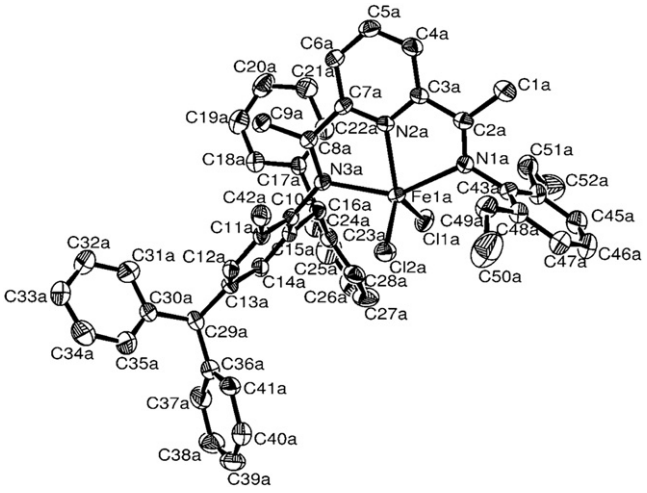

Fig. 2. ORTEP drawing of complex **C2** with thermal ellipsoids at 30% probability level (two independent molecules are included, only one structure is listed). Hydrogen atoms have been omitted for clarity. Selected bond length (°) and selected bond angles (Å): Fe(1)-N(1) 2.279(5), Fe(1)-N(2) 2.111(4), Fe(1)-N(3) 2.267(5), Fe(1)-Cl(1) 2.290(2), Fe(1)-Cl(2) 2.2902 (19), N(1)-C(2) 1.266(7), N(1)-C(43) 1.464(7), N(2)-C(3) 1.331(7), N(2)-C(7) 1.360(7), N(3)-C(8) 1.298(7), N(3)-C(10) 1.440(7), N(2)-Fe(1)-N(1) 72.52(18), N(2)-Fe(1)-Cl(1) 121.0839(14), N(3)-Fe(1)-Cl(1) 101.12(13), N(2)-Fe(1)-N(3) 73.89(17), N(1)-Fe(1)-N(3) 146.41(17), N(1)-Fe(1)-Cl(1) 96.78(13), N(2)-Fe(1)-Cl(2) 122.56(14), N(3)-Fe(1)-Cl(2) 98.82(14), Cl(1)-Fe(1)-Cl(2) 115.96(7), N(1)-Fe(1)-Cl(2) 98.52(14).

reaction temperature. With regard to the influence shown by different co-catalysts, the discussion regarding ethylene polymerization is divided into two parts, *viz* i) use of methylaluminoxane (MAO) and ii) use of modified methylaluminoxane (MMAO).

3.2.1. Ethylene polymerization in the presence of the co-catalyst MAO

The iron complex **C5** was used to optimize the reaction conditions and the parameters of ethylene pressure, the molar ratio of Al/Fe, reaction temperature and the lifetime of the active species were varied. The results are tabulated in Table 2.

Under an ambient pressure of ethylene with Al/Fe at 3000 (entries 1–3, Table 2), the catalytic activities were sensitive to the reaction temperature with the optimum temperature observed as 40 °C (entry 2, Table 2). In addition, the polyethylene (PE) obtained at 40 °C had a narrow molecular weight distribution, indicating the promising property of these iron systems behaving as single-site catalysts.

Inspired by previous observations of "higher ethylene pressure, better catalytic activity" [20,42,60], the trials of various Al/Fe molar ratios were conducted by employing an ethylene pressure of 10 atm at 20 °C (entries 4–7, Table 2). Similar activities were observed on changing the Al/Fe molar ratios, but the optimum activity was achieved at Al/Fe 3000. DSC and GPC measurements of the resultant polyethylene products were carried out, and the values of the melting points and molecular weights were found to be quite random. Upon closer inspection of the GPC curves of the resultant polyethylenes (Fig. 3), it was observed that for the polyethylenes obtained, the major portions were of high molecular weight and the minor portions of low molecular weight at Al/Fe 1000, whilst more polyethylenes with low molecular weights were produced on increasing the molar ratio of Al/Fe (to 2000 and 3000).

The multi-modal polyethylenes formed were consistent with multiple active centers operating [46, 61]. The GPC chart of the polyethylene obtained at the molar ratio of Al/Fe 2000 (entry 5, Table 2) can be separated into four curves [**A** with peak at $M_w = 238$, **B** with peak at $M_w = 1023$, **C** with peak at $M_w = 23{,}575$, and **D** with peak at $M_w = 264{,}472$, with respective intensities of **A** (12%), **B** (32%), **C** (32%), and **D** (24%)] (Fig. 4). These separated curves showed four fractions of polyethylenes formed as tetra-modal features, thought to be caused by at least four types of different active species operating in the catalytic system. Although it was not the most active system at Al/Fe 4000, the GPC curve of the resultant polyethylene did show unique narrow molecular distribution. Such an observation indicated a possible promising way of re-optimization of the reaction parameter for tuning the active species.

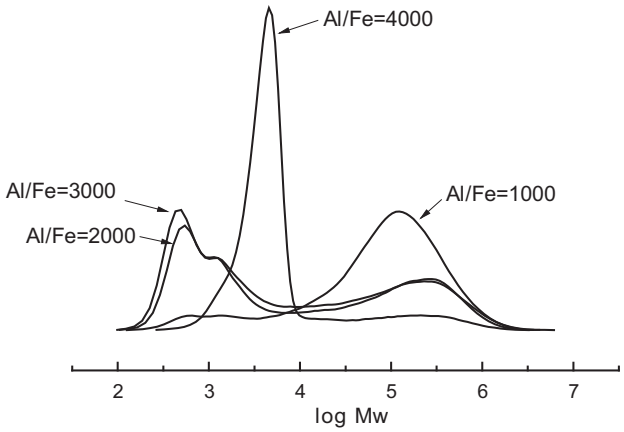

Fig. 3. The GPC curves of the polyethylenes (entries 4–7, Table 2).

On the basis that the most effective catalysis was observed at 10 atm ethylene and the Al/Fe 3000, under these conditions, variation of the reaction temperature was conducted up to 100 °C with the pre-catalyst **C5** (entries 6, 8–11, Table 2); the GPC curves of the resultant polyethylenes are illustrated in Fig. 5. It was clear that there were more polyethylenes with high molecular weights produced at lower reaction temperatures (entry 6 at 20 °C, and entry 8 at 40 °C, Table 2). Single-site species were achieved at elevated reaction temperatures (entry 9 at 60 °C, and entry 10 at 80 °C, Table 2) [20,46,62,63], however, further increasing the reaction temperature induced the formation of multiple active centers, and produced polyethylene products with the major portion being of lower molecular weight (entry 11 at 100 °C, Table 2). Accordingly, three sets of active species are promising here, two sets of species at low reaction temperature produced, as the major product, polymer with high molecular weight and minor polymer with low molecular weight, and two sets of species at high reaction temperature produced major polymer with low molecular weight and minor polymer with 'mid' molecular weight, and the likely single-site species operating around 60 °C and 80 °C formed polymer with 'mid' molecular weight. The most effective catalysis was conducted at 60 °C, and produced polyethylene products with

Table 2
Ethylene polymerization by **C5**/MAO.[a]

Entry	Pressure (atm)	Al/Fe	T (°C)	t (min)	PE (g)	Activity[b]	M_w[c] (kg mol^{-1})	M_w/M_n[c]	T_m[d] (°C)
1	1	3000	20	30	0.50	0.66	30.1	7.3	122.4
2	1	3000	40	30	0.94	1.25	1.4	1.4	116.3
3	1	3000	60	30	Trace	Trace	–	–	–
4	10	1000	20	30	2.91	3.88	187.6	22.8	128.1
5	10	2000	20	30	2.95	3.94	127.0	88.6	126.3
6	10	3000	20	30	3.20	4.27	112.7	97.7	123.9
7	10	4000	20	30	2.80	3.73	39.4	10.5	126.3
8	10	3000	40	30	11.76	15.7	43.6	14.0	128.1
9	10	3000	60	30	15.68	20.9	11.8	3.2	127.1
10	10	3000	80	30	11.71	15.6	10.1	3.0	126.1
11	10	3000	100	30	0.46	6.13	3.9	7.3	117.3
12	10	3000	60	5	6.53	52.2	3.5	1.3	123.8
13	10	3000	60	10	10.54	42.2	4.6	1.3	126.1
14	10	3000	60	20	14.27	28.5	5.6	1.3	126.8
15	10	3000	60	60	21.87	14.6	4.0	9.3	129.1

[a] General conditions: 1.5 μmol of Fe; 30 mL toluene for 1 atm ethylene, and 100 mL toluene for 10 atm ethylene.
[b] 10^6 g mol^{-1}(Fe) h^{-1}.
[c] Determined by GPC.
[d] Determined by DSC.

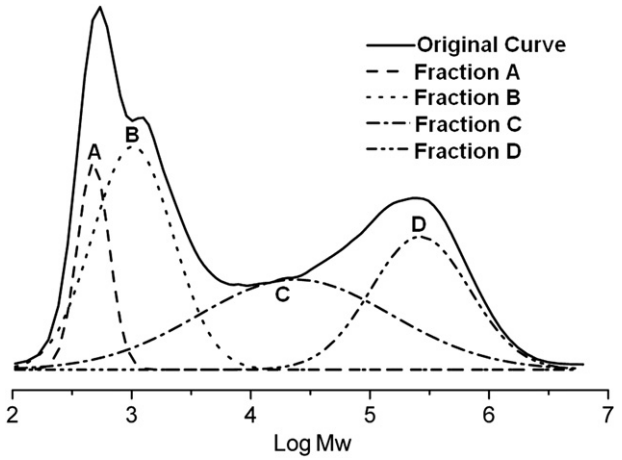

Fig. 4. The tetra-modal feature of the polyethylene GPC curve (entry 5, Table 2).

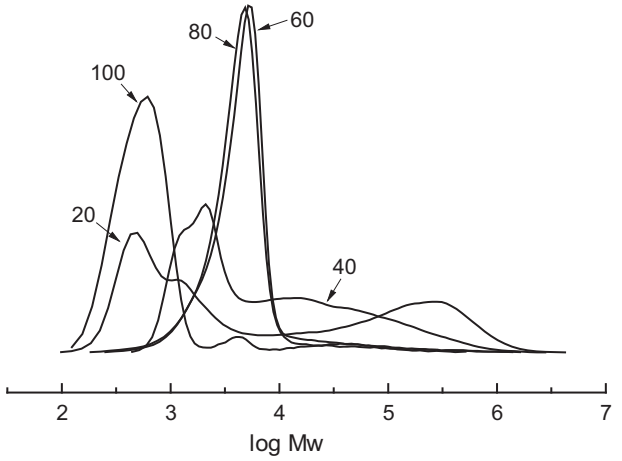

Fig. 5. The GPC curves of polyethylenes obtained at variant temperatures (°C) (entries 6, 8–11, Table 2).

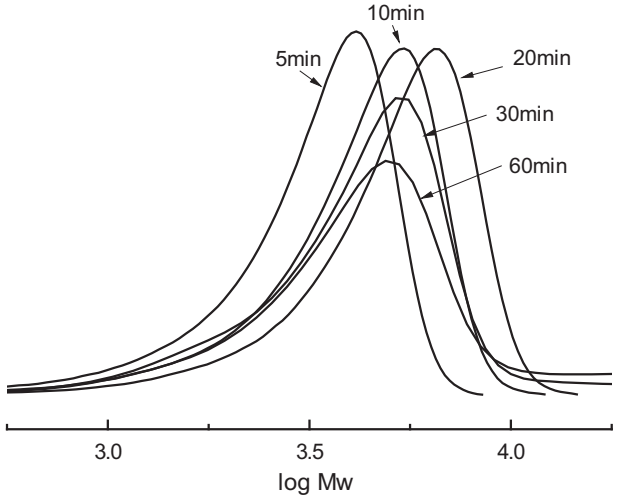

Fig. 6. The GPC curves of the polyethylenes obtained at different reaction periods (Entries 9 and 12–15, Table 2).

Table 3
Ethylene polymerization with **C1**–**C5**/MAO.[a]

Entry	Cat.	Act.[b]	M_w[c] (kg mol^{-1})	M_w/M_n[c]	T_m[d] (°C)
1	**C1**	18.5	11.4	3.8	126.3
2	**C2**	17.4	17.2	6.1	127.4
3	**C3**	26.2	18.7	4.4	128.4
4	**C4**	24.7	11.4	2.8	128.1
5	**C5**	20.9	11.8	3.2	127.1

[a] General conditions: 1.5 μmol of Fe; 3000 of Al/Fe; 100 mL toluene; 60 °C; 30 min.
[b] 10^6 g mol^{-1}(Fe) h^{-1}.
[c] Determined by GPC.
[d] Determined by DSC.

narrow molecular weights, indicating a single-site active species in the catalytic system.

To understand the lifetime of the catalytic species, the catalytic system of **C5**/MAO, under 10 atm ethylene and with Al/Fe 3000 at 60 °C, was quenched at different reaction periods (entries 9, 12–15, Table 2). More polyethylene was formed on prolonging the reaction time, however, the observed activities decreased, indicative of little or no induction period. The catalytic activities sharply decreased over 20–30 min (entries 13 and 14, Table 2), but the catalytic species did remain active (entry 15, Table 2). The GPC curves of the resultant polyethylenes indicated chain propagation and well maintained single-site active species were present at 20 min, however, multiple active centers formed on further prolonging the reaction time, and this resulted in polyethylenes with wide molecular weight distributions (Fig. 6). It could be imagined that a second species formed from the decaying single-site active species is operating during this catalysis.

Using the optimum reaction conditions of Al/Fe 3000 at 60 °C over 30 min, all the iron pre-catalysts were investigated for their ethylene polymerization capability, and it was found that they showed extremely high activity (Table 3). The pre-catalyst (**C2**) (entry 2, Table 3) with R^1 as ethyl group gave polyethylenes with wider molecular weight distributions than polyethylenes produced by the analogs **C1** and **C3** (entries 1 and 3, Table 3), possibly caused by the flexibility of the rotation within the ethyl group. The pre-catalysts **C4** and **C5** (entries 4 and 5, Table 3) having an additional R^2 (methyl) group showed higher activities than did the analogs **C1** and **C2** (entries 1 and 2, Table 3), indicating a positive effect of an addition methyl group in such ligands [64].

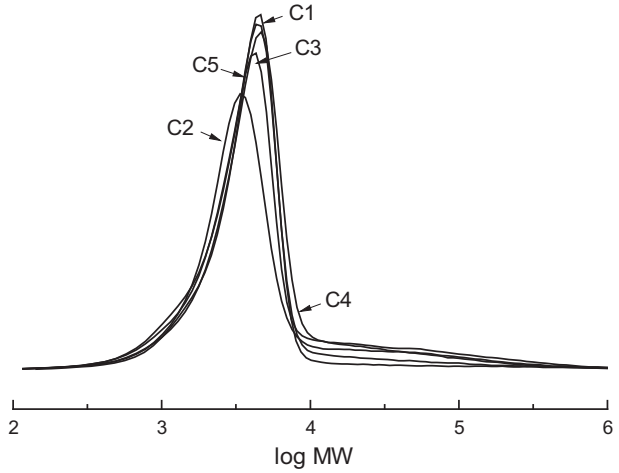

Fig. 7. The GPC curves of polyethylenes obtained by pre-catalysts **C1**–**C5** (Table 3).

Table 4
Catalytic results of ethylene polymerization with **C1**–**C5**/MMAO.[a]

Entry	Cat.	Cocat.	Pres. (atm)	Al/Fe	T (°C)	t (min)	PE (g)	Act.[b]	M_w[c] (kg·mol^{-1})	M_w/M_n[c]	T_m[d] (°C)
1	C5	MMAO	1	3000	20	30	0.46	0.61	11.8	18.4	122.6
2	C5	MMAO	1	3000	30	30	1.85	2.46	4.0	3.6	121.3
3	C5	MMAO	1	3000	40	30	1.64	2.19	1.2	1.2	88.8
4	C5	MMAO	1	3000	50	30	1.11	1.47	1.1	1.3	87.9
5	C5	MMAO	1	3000	60	30	0.32	0.43	0.6	1.2	71.9
6	C5	MMAO	10	1000	20	30	1.84	2.45	208.0	69.8	133.9
7	C5	MMAO	10	2000	20	30	4.01	5.34	21.5	12.2	125.8
8	C5	MMAO	10	3000	20	30	6.30	8.40	17.5	10.7	125.8
9	C5	MMAO	10	4000	20	30	3.63	4.84	4.6	3.9	118.9
10	C5	MMAO	10	3000	40	30	7.96	10.6	30.6	13.6	124.0
11	C5	MMAO	10	3000	60	30	14.27	19.0	10.8	3.5	125.8
12	C5	MMAO	10	3000	70	30	17.47	23.3	12.1	3.5	127.6
13	C5	MMAO	10	3000	80	30	4.65	6.20	2.5	1.4	116.0
14	C1	MMAO	10	3000	70	30	17.02	22.7	18.1	5.1	128.0
15	C2	MMAO	10	3000	70	30	15.08	20.1	23.7	28.2	128.0
16	C3	MMAO	10	3000	70	30	14.98	20.0	13.9	4.5	126.3
17	C4	MMAO	10	3000	70	30	15.70	20.9	14.3	4.3	126.6

[a] General conditions: 1.5 μmol of Fe; 30 mL toluene for 1 atm ethylene, and 100 mL toluene for 10 atm ethylene.
[b] 10^6 g mol^{-1}(Fe) h^{-1}.
[c] Determined by GPC.
[d] Determined by DSC.

The melting points of the resultant polyethylenes, with close values, indicated highly linear polyethylene products were formed. The GPC curves of the resultant polyethylenes, with either narrow or wide molecular weight distributions, showed only mono-modal features (Fig. 7). Therefore, the newly developed iron pre-catalysts are promising in producing (semi-)single-site active species and potentially useful polyethylene materials.

*3.2.2. Ethylene polymerization with the **C1**–**C5**/MMAO systems*

All the iron pre-catalysts were also investigated using MMAO as the co-catalyst, and the results are tabulated in Table 4. Employing the same procedures as for the catalytic system **C5**/MAO, the influence of the reaction temperature on the activities of the **C5**/MMAO system indicated the optimum value of 30 °C under ambient pressure (entries 1–5, Table 4). Under 10 atm ethylene, results were consistent with an optimum Al/Fe ratio of 3000 for the most effective polymerization (entry 8, Table 4), though on changing of the molar ratios of Al/Fe (entries 6–9, Table 4), the polymer molecular weight distribution more closely approached that of single-site catalysis at Al/Fe 4000. The molecular weights of the resultant polyethylenes gradually decreased on increasing the Al/Fe molar ratios, consistent with the observation of enhanced chain transfer to aluminum at the high Al/Fe molar ratio [20,46,65–67]. In regard to the influence of the reaction temperature (entries 8 and 10–14, Table 4), the highest activity was obtained at 70 °C (entry 12, Table 4), indicating enhanced thermostability in the presence of MMAO than for that observed in the presence of MAO. The polyethylene obtained at 80 °C was of low molecular weight and quite narrow molecular weight distribution, and moreover, the catalytic system gave very low activity.

Employing the optimum conditions, namely 10 atm ethylene at 70 °C over 30 min, all the iron pre-catalysts showed very high activities for ethylene polymerization (entries 12 and 14-17 in Table 4). Again, pre-catalysts **C4** and **C5** (entries 12 and 17 in Table 4) performed with slightly higher activities than did their analogs **C1** and **C2** (entries 14 and 15 in Table 4). Affected by the presence of bulky *t*-butyl group in MMAO, the catalytic activities decreased in the order of **C1** > **C2** > **C3** due to the steric bulkiness of the ligands [8,34,35,68]. Comparison of the data in Tables 3 and 4, indicates that the catalytic systems utilizing MMAO generally showed lower activities and produced polyethylenes with lower molecular weights than those employing MAO, which is consistent with the observation of considering MMAO as a better chain transfer agent [69]. (GPC curves of the polyethylenes obtained with the co-catalyst MMAO are given as supplementary material).

4. Conclusion

A series of iron(II) complexes bearing bulky unsymmetrical 2,6-bis(imino)pyridines was synthesized and fully characterized. All pre-catalysts **C1**–**C5** performed with very high activities for ethylene polymerization at 60 °C in the presence of MAO, and at 70 °C in the presence of MMAO under 10 atm ethylene. The polyethylenes obtained could be adaptable for multi-modal or mono-modal features, and polyethylenes with quite narrow molecular weight distributions were obtained. Moreover, the molecular weights of the polyethylenes could be tuned from thousands to hundreds of thousands. The reaction temperatures (60 °C and 70 °C) are heading toward those required for industrial operation, and the resultant polyethylenes are promising in terms of further functionalization and application.

Acknowledgments

This work is supported by MOST 863 program No. 2009AA034601. CR thanks the EPSRC for the awarded travel grant.

Appendix. Supplementary material

Supplementary data related to this article can be found online at doi:10.1016/j.polymer.2011.11.024.

References

[1] Small BL, Brookhart M, Bennett AMA. J Am Chem Soc 1998;120(16):4049–50.
[2] Britovsek GJP, Gibson VC, Kimberley BS, Maddox PJ, McTavish SJ, Solan GA, et al. Chem Commun 1998;7:849–50.
[3] Britovsek GJP, Gibson VC, Wass DF. Angew Chem Int Ed 1999;38(4):428–47.
[4] Ittel SD, Johnson LK, Brookhart M. Chem Rev 2000;100(4):1169–203.
[5] Gibson VC, Spitzmesser SK. Chem Rev 2003;103(1):283–315.
[6] Bianchini C, Giambastiani G, Rios IG, Mantovani G, Meli A, Segarra AM. Coord Chem Rev 2006;250(11–12):1391–418.
[7] Gibson VC, Redshaw C, Solan GA. Chem Rev 2007;107(5):1745–76.
[8] Sun WH, Zhang S, Zuo WW. Compt Rendus Chim 2008;11(3):307–16.
[9] Gupta KC, Sutar AK. Coord Chem Rev 2008;252(12–14):1420–50.

[10] Jie S, Sun WH, Xiao T. Chin J Polym Sci 2010;28(3):299–304.
[11] Bianchini C, Giambastiani G, Luconi L, Meli A. Coord Chem Rev 2010; 254(5–6):431–55.
[12] Xiao T, Zhang W, Lai J, Sun WH. Compt Rendus Chim 2011;14(10):851–5.
[13] Gibson VC, Humphries MJ, Tellmann KP, Wass DF, White AJP, Williams DJ. Chem Commun 2001;21:2252–3.
[14] Ma Z, Sun WH, Li Z, Shao C, Hu Y, Li X. Polym Int 2002;51(10):994–7.
[15] Bianchini C, Mantovani G, Meli A, Migliacci F, Zanobini F, Laschi F, et al. Eur J Inorg Chem 2003;8:1620–31.
[16] Bluhm ME, Folli C, Döring M. J Mol Catal A Chem 2004;212(1–2):13–8.
[17] Chen YF, Qian CT, Sun J. Organometallics 2003;22(6):1231–6.
[18] Zhang T, Sun WH, Li T, Yang X. J Mol Catal A Chem 2004;218(2):119–24.
[19] Wallenhorst C, Kehr G, Luftmann H, Fröhlich R, Erker G. Organometallics 2008;27(24):6547–56.
[20] Yu J, Liu H, Zhang W, Hao X, Sun WH. Chem Commun 2011;47(11):3257–9.
[21] Guo LH, Gao HY, Zhang L, Zhu FM, Wu Q. Organometallics 2010;29(9):2118–25.
[22] Deng LQ, Margl P, Ziegler T. J Am Chem Soc 1999;121(27):6479–87.
[23] Talsi EP, Babushkin DE, Semikolenova NV, Zudin VN, Panchenko VN, Zakharov VA. Macromol Chem Phys 2001;202(10):2046–51.
[24] Khoroshun DV, Musaev DG, Vreven T, Morokuma K. Organometallics 2001; 20(10):2007–26.
[25] Britovsek GJP, Clentsmith GKB, Gibson VC, Goodgame DML, McTavish SJ, Pankhurst QA. Catal Commun 2002;3(5):207–11.
[26] Bryliakov KP, Semikolenova NV, Zakharov VA, Talsi EP. Organometallics 2004; 23(22):5375–8.
[27] Bryliakov KP, Semikolenova NV, Zudin VN, Zakharov VA, Talsi EP. Catal Commun 2004;5(1):45–8.
[28] Bryliakov KP, Talsi EP, Semikolenova NV, Zakharov VA. Organometallics 2009; 28(11):3225–32.
[29] Cruz VL, Ramos J, Martinez-Salazar J, Gutierrez-Oliva S, Toro-Labbe A. Organometallics 2009;28(20):5889–95.
[30] Trovitch RJ, Lobkovsky E, Chirik PJ. J Am Chem Soc 2008;130(35):11631–40.
[31] Wang L, Sun WH, Han L, Yang H, Hu Y, Jin X. J Organomet Chem 2002; 658(1–2):62–70.
[32] Britovsek GJP, Baugh SPD, Hoarau O, Gibson VC, Wass DF, White AJP, et al. Inorg Chim Acta 2003;345:279–91.
[33] Sun WH, Tang X, Gao T, Wu B, Zhang W, Ma H. Organometallics 2004;23(21): 5037–47.
[34] Sun WH, Jie S, Zhang S, Zhang W, Song Y, Ma H. Organometallics 2006;25(3): 666–77.
[35] Jie S, Zhang S, Sun WH, Kuang X, Liu T, Guo J. J Mol Catal A Chem 2007; 269(1–2):85–96.
[36] Chen Y, Hao P, Zuo W, Gao K, Sun WH. J Organomet Chem 2008;693(10): 1829–40.
[37] Xiao L, Gao R, Zhang M, Li Y, Cao X, Sun WH. Organometallics 2009;28(7): 2225–33.
[38] Sun WH, Hao P, Zhang S, Shi Q, Zuo W, Tang X, et al. Organometallics 2007; 26(10):2720–34.
[39] Beaufort L, Benvenuti F, Noels AF. J Mol Catal A Chem 2006;260(1–2):210–4.
[40] Zhang M, Zhang W, Xiao T, Xiang J, Hao X, Sun WH. J Mol Catal A Chem 2010; 320(1–2):92–6.
[41] Gao R, Li Y, Wang F, Sun WH, Bochmann M. Eur J Inorg Chem 2009;27(27): 4149–56.
[42] Zhang S, Sun WH, Xiao T, Hao X. Organometallics 2010;29(5):1168–73.
[43] Appukuttan V, Liu Y, Son B, Ha C, Suh H, Kim I. Organometallics 2011;30(8): 2285–94.
[44] Xiao T, Zhang S, Li B, Hao X, Redshaw C, Li YS, et al. Polymer 2011;52(25): 5803–10.
[45] Xiao T, Zhang S, Kehr G, Hao X, Erker G, Sun WH. Organometallics 2011;30: 3658–65.
[46] Song S, Zhao W, Wang L, Redshaw C, Wang F, Sun WH. J Organomet Chem 2011;696(18):3029–35.
[47] Song S, Xiao T, Redshaw C, Hao X, Wang F, Sun WH. J Organomet Chem 2011; 696(13):2594–9.
[48] Britovsek GJP, Mastroianni S, Solan GA, Baugh SPD, Redshaw C, Gibson VC, et al. Chem Eur J 2000;6(12):2221–31.
[49] Small BL, Brookhart M. J Am Chem Soc 1998;120(28):7143–4.
[50] Britovsek GJP, Bruce M, Gibson VC, Kimberley BS, Maddox PJ, Mastroianni S, et al. J Am Chem Soc 1999;121(38):8728–40.
[51] Fernandes S, Bellabarba RM, Ribeiro AF, Gomes PT, Ascenso JR, Mano JF, et al. Polym Int 2002;51(12):1301–3.
[52] Paulino IS, Schuchardt U. J Mol Catal A Chem 2004;211(1–2):55–8.
[53] Yu J, Hu X, Zeng Y, Zhang L, Ni C, Hao X, et al. New J Chem 2011;35(1): 178–83.
[54] Brasse M, Campora J, Palma P, Alvarez E, Cruz V, Ramos J, et al. Organometallics 2008;27(18):4711–23.
[55] McGuinness DS, Gibson VC, Steed JW. Organometallics 2004;23(26):6288–92.
[56] Ishii S, Mitani M, Saito J, Matsuura S, Kojoh S, Kashiwa N, et al. Chem Lett 2002;7:740–1.
[57] Sainath AVS, Isokawa M, Suzuki M, Ishii S, Matsuura S, Nagai N, et al. Macromolecules 2009;42(13):4356–8.
[58] Terao H, Ishii S, Saito J, Matsuura S, Mitani M, Nagai N, et al. Macromolecules 2006;39(25):8584–93.
[59] Sheldrick GM. SHELXL-97, program for the refinement of crystal structures. Germany: University of Göttingen; 1997.
[60] Hao P, Zhang S, Sun WH, Shi Q, Adewuyi S, Lu X, et al. Organometallics 2007; 26(9):2439–46.
[61] Wang Q, Li L, Fan Z. Eur Polym J 2004;40(8):1881–6.
[62] Barabanov AA, Bukatov GD, Zakharov VA, Semikolenova NV, Mikenas TB, Echevskaja LG, et al. Macromol Chem Phys 2006;207(15):1368–75.
[63] Barbanov AA, Bukatov GD, Zakharov VAJ. Polym Sci A Polym Chem 2008; 46(19):6621–9.
[64] Liu JY, Zheng Y, Li YG, Pan L, Li YS, Hu NH. J Organomet Chem 2005;690(5): 1233–9.
[65] Sun WH, Hao P, Li G, Zhang S, Wang W, Yi J, et al. J Organomet Chem 2007; 692(21):4506–18.
[66] Wang S, Liu D, Huang R, Zhang Y, Mao B. J Mol Catal A Chem 2006;245(1–2): 122–31.
[67] Campora J, Naz AM, Palma P, Alvarez E, Reyes ML. Organometallics 2005; 24(20):4878–81.
[68] Hao P, Chen Y, Xiao T, Sun WH. J Organomet Chem 2010;695(1):90–5.
[69] Chen EYX, Marks TJ. Chem Rev 2000;100:1391–434.